MINERALOGICAL MAGAZINE, SEPTEMBER 1970, VOL. 37, NO. 291

Nucleation and growth of iron oxides in olivines, $(Mg,Fe)_2SiO_4$

P. E. CHAMPNESS
Department of Geology, University of Manchester

SUMMARY. Iron-rich olivines have been oxidized in air in the laboratory and the mechanism of their breakdown has been elucidated using X-ray diffraction and electron microscopy. Low-temperature oxidation (500–800 °C) produces well-oriented hematite- and magnetite-like precipitates together with amorphous silica. The reaction is a cellular one in which thin needles of oxide about 50–100 Å apart grow into the matrix separated by regions of amorphous silica. Nucleation of spherical colonies of the iron oxide and silica occurs on dislocations.

Although the hematite or magnetite always shows the same topotactic relationship with the matrix, the direction in which the needle-like precipitates grow is determined by the orientation of the nucleating dislocation. The small size and highly distorted nature of these precipitates accounts for the diffuseness of their X-ray reflections.

Oxidation at 1000 °C produces undistorted equiaxed grains of the oxides about 0·2 μm in size. They are surrounded by silica, which produces a disordered electron diffraction pattern. As the temperature is raised, the silica achieves more structural order and the oxide grains increase in size.

THE common rock-forming mineral olivine forms a complete solid solution between forsterite, Mg_2SiO_4, and fayalite, Fe_2SiO_4. It is an orthosilicate (i.e. it contains individual SiO_4 tetrahedra) in which the oxygen ions are approximately hexagonal close-packed parallel to (100). The magnesium and iron ions are sixfold coordinated by oxygen and occupy half of the available sites, forming zigzag chains of octahedra along [001], while silicon occupies one-eighth of the available fourfold sites.

Forsterite has been used as a refractory in the ceramic and metallurgical industries and the fact that solid solution of the ferrous end member not only reduces the melting point of the refractory but also introduces complexities by oxidation, together with the importance of olivine alteration in rocks, has led to studies of olivine oxidation in the past.[1]

Koltermann (1962) investigated the atmospheric oxidation of powdered olivines containing 11, 34, and 53 % fayalite by X-ray powder diffraction and infra-red spectroscopy. His results for the 53 % fayalite specimen may be briefly summarized:

$$(Mg,Fe)_2SiO_4 \xrightarrow[820\ ^\circ C]{\text{fast reaction}} \underset{\text{forsterite}}{Mg_2SiO_4}, \quad \underset{\text{amorphous silica}}{SiO_2}, \quad \underset{\text{hematite}}{Fe_2O_3}$$

$$\xrightarrow[1080\ ^\circ C]{\text{fast reaction}} \underset{\text{cristobalite}}{SiO_2}, \quad Mg_2SiO_4, \quad \underset{\text{enstatite}}{MgSiO_3}, \quad Fe_2O_3$$

$$\xrightarrow[1100\ ^\circ C]{\text{with prolonged heating}} Mg_2SiO_4, \quad \underset{\text{cristobalite}}{SiO_2}, \quad MgSiO_3, \quad \underset{\text{magnetite}}{Fe_3O_4}$$

[1] Gorgeu (1885), Hugill and Green (1938), Weiskirchner (1958), Koltermann (1962), Koltermann and Mueller (1963), Haggerty and Baker (1967), Champness (1968), Champness and Gay (1968).

Koltermann and Mueller (1963) made further studies on the oxidation of powdered olivines, including fayalite, using differential thermal analysis and X-ray powder diffraction. Their results were similar to those described by Koltermann (1962).

Recently Haggerty and Baker (1967) have studied the high-temperature oxidation of olivines in basaltic and associated lavas by means of reflection microscopy and X-ray powder diffraction. To supplement these observations, they carried out heating experiments in air at 600–1000 °C on powdered and single-crystal samples of composition 20 % fayalite. In the powdered samples forsterite and hematite formed at all temperatures, no silica or enstatite being detected by X-rays.

In the single crystals, magnetite was also detected after oxidation at low temperatures and a phase resembling enstatite was precipitated at all temperatures from 820 to 1000 °C. The enstatite disappeared on further heating at 950 °C, presumably forming forsterite and silica.

Champness and Gay (1968) reported preliminary results of a study of olivine oxidation in which X-ray single crystal and powder methods, infra-red spectroscopy, and transmission electron microscopy were used. This paper is a more detailed account of part of that work.

The specimens used for this investigation were a fayalite containing no magnesium (specimen no. 1184 in the mineral collection, Department of Mineralogy and Petrology, University of Cambridge) from Rockport, Massachusetts (Bowen *et al.*, 1933) and two hortonolites, no. 39126 from Camas Mor, Muck, with composition 52·2 mol % fayalite (Tilley, 1952) and no. 54087 (rock collection, Department of Mineralogy and Petrology, Cambridge) from the Bushveld Complex, South Africa. The spacing of the 130 line on a powder diffractometer trace (Yoder and Sahama, 1957) gave the approximate composition of the latter hortonolite as 47 mol % fayalite.

Precipitation of iron oxides and silica

For X-ray studies, hand-picked unaltered grains were heated in air in a vertical furnace in which the temperature was constant to within ± 5 °C.

Oxides. Single crystal oscillation photographs showed that the main product of oxidation of iron-rich olivines between 200 and 800 °C is a hematite-like phase in twinned orientation with respect to the host: $a_{ol} \parallel c_h$; $b_{ol} \parallel \pm b_h$; $c_{ol} \parallel \pm [210]_h$. In the early stages of the reaction a twinned spinel-like phase is precipitated with the orientation $a_{ol} \parallel [111]_{sp}$; $b_{ol} \parallel \pm [\bar{1}\bar{1}2]_{sp}$; $c_{ol} \parallel \pm [1\bar{1}0]_{sp}$.

It seems probable that the composition of the spinel phase, at least for a reaction temperature above 900 °C, is near to that of magnetite, Fe_3O_4, although it may contain a little magnesium in solid solution. Measurement of the high-angle line 751 on a powder photograph of olivine no. 54087 heated for three days at 1200 °C gave a 8·393±0·002 Å, the value for pure Fe_3O_4 (Deer, Howie, and Zussman, 1962). However, in view of the variation in the quoted values for synthetic magnesioferrite (Holgersson, 1927, gives 8·34 Å and Posnjak, 1930, gives 8·383 Å), the cell dimension may not be a reliable guide to the magnesium content of the spinel.

Topotaxy of both oxide phases in the olivine matrix is good although the spinel is

less well oriented than the hematite (fig. 1). Both spinel and hematite have planes of approximately close-packed oxygens; on this basis the preferred orientation is readily interpreted in terms of diffusion of cations within a relatively unchanged oxygen framework. In hematite the oxygen planes are approximately hexagonal close-packed parallel to (0001) and the Fe^{3+} occupy $\frac{2}{3}$ of the six-fold interstices in each cation layer parallel to (0001).

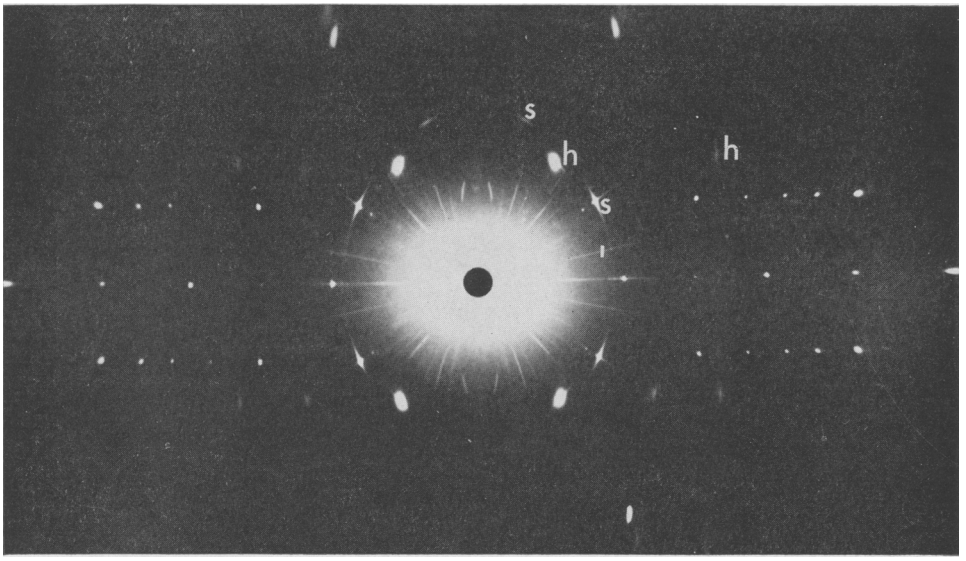

FIG. 1. X-ray oscillation photograph of a 53 mol % olivine that was heated for three days at 670 °C. The sharp reflections are olivine and hematite, and spinel reflections are marked h and s respectively.

The spinel structure has approximately cubic close-packed oxygen planes parallel to {111}. Two kinds of cation layers alternate between the oxygen planes: the 'kagome' layer has metal atoms in $\frac{3}{4}$ of the six-fold sites and the 'mixed-trigonal' layer has $\frac{1}{4}$ of the four-fold and $\frac{1}{4}$ of the six-fold sites occupied. The transformation of olivine to spinel involves the change from hexagonal to cubic close-packed oxygen planes as well as diffusion of cations. Such change of packing can take place by slip on the close-packed planes with every two of the layers locked together (Venables, 1962). The shear process occurs by the passage of partial dislocations.

The X-ray reflections from the oxide phases precipitated below 900 °C are extremely diffuse (fig. 1). Above this temperature the reflections sharpen gradually and at 1000 °C coarsening of the precipitates occurs (the powder rings become spotty). The diffuseness at low temperatures affects all the reflections of the oxides and does not appear to depend on the distance of the diffraction maximum concerned from the origin of reciprocal space. Diffuse reflections of the kind observed here are indicative of disordered or imperfect precipitates, but X-ray diffraction methods cannot, in general, distinguish between the various kinds of imperfection.

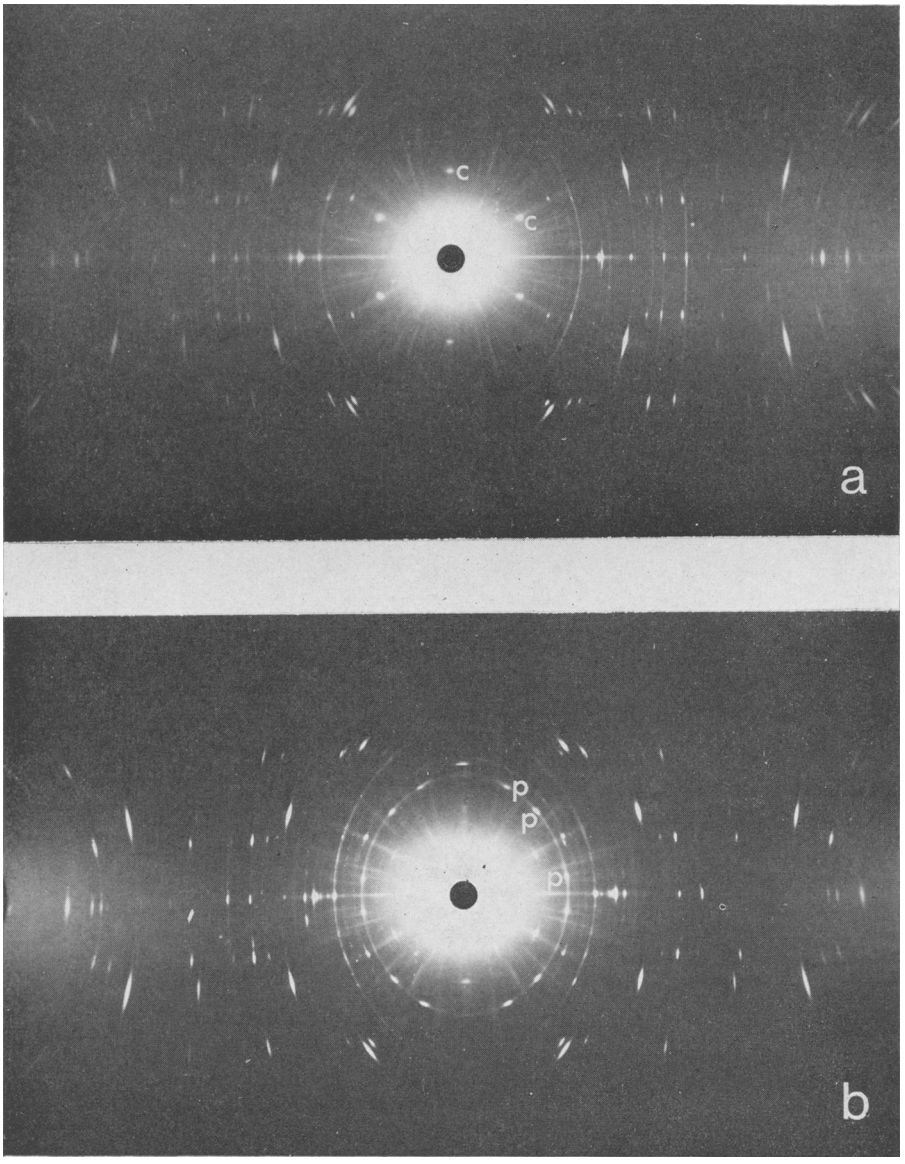

FIG. 2 *a*, Oscillation photograph of a 47 mol % fayalite crystal heated for three days at 1000 °C, *c*-axis across *a**. Six diffuse reflections from a cristobalite-like phase are marked c. *b*, A similar crystal heated for one day at 1100 °C, *c*-axis across *a**. The silica reflections are accompanied by twelve pyroxene reflections (marked p).

Silica. Heating single crystals of both forsteritic and fayalitic olivines in air for three days at 900 °C and above produces six diffuse X-ray reflections that can be attributed to silica (fig. 2*a*). Although the topotaxy is not as good as in the case of the iron

oxides, the reflections can be indexed as a cristobalite-like phase with the orientation: $(100)_{ol} \| (111)_{crist}$; $b_{ol} \| [1\bar{1}0]_{crist}$. The zone repeats are consistent with the dimensions *a* 7·02, *c* 6·92 Å for a tetragonal[1] unit cell (Jay, 1944).

There is a second orientation that sometimes occurs with the first, $(100)_{ol} \| (111)_{crist}$; $b_{ol} \| \pm[\bar{1}\bar{1}2]_{crist}$.

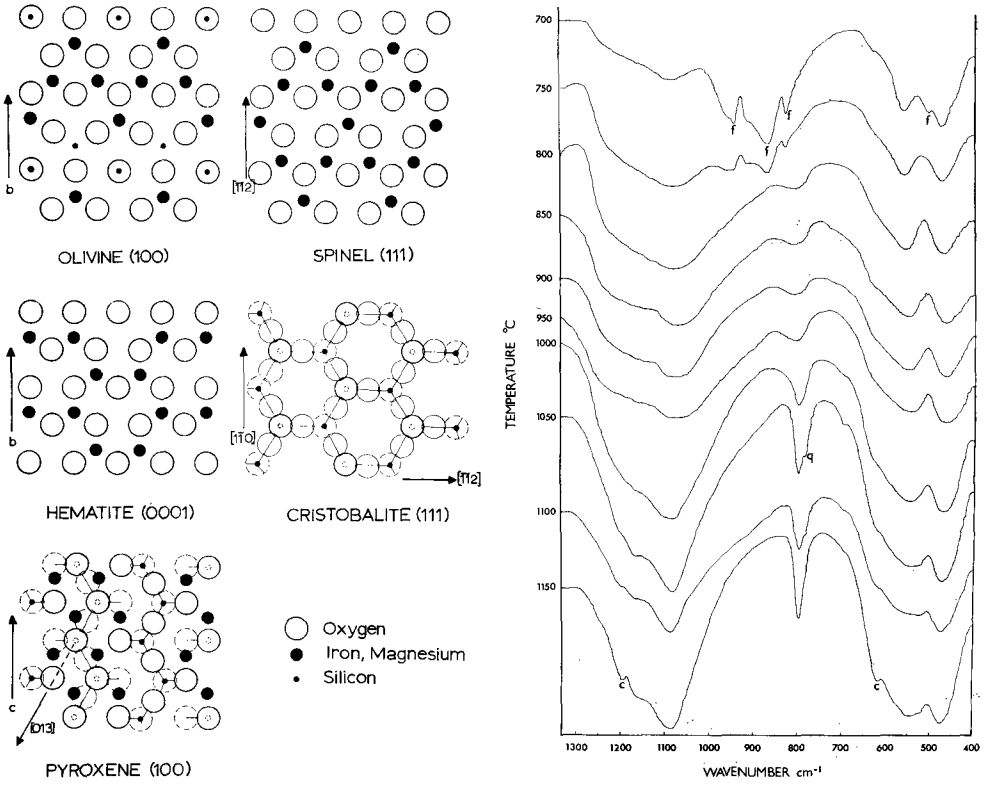

FIGS. 3 and 4: Fig. 3. The idealized orientations of olivine and its breakdown products. Idealized partial projections. Fig. 4. Infra-red spectra of fayalite samples heated in air for three days at temperatures from 700 to 1150 °C. Heating at 700 and 750 °C results in incomplete oxidation (the fayalite peaks are marked f). q is the diagnostic peak of quartz and the two peaks marked c are diagnostic of cristobalite.

Although the oxygen planes in cristobalite are not densely packed, their stacking along [111] to some extent resembles hexagonal close-packing. The moderate preferred orientation of the cristobalite-like phase in olivine is readily explained by this fact; both $[1\bar{1}0]$ and $[\bar{1}\bar{1}2]$ of cristobalite are directions that are structurally similar to [010] of olivine (fig. 3).

A small amount of quartz can also be detected as an oxidation product of olivine.

[1] The *C*-face centred cell is used here in order to conform with the axes of the high-temperature, cubic form.

It appears to occur as an early phase and to be later replaced by cristobalite. It is unoriented in the olivine matrix, presumably because of the dissimilarity between the two structures.

Oxidation of olivines at temperatures below that at which silica crystallizes produces an amorphous silica phase. The variation in crystallinity of the silica was followed by comparing infra-red spectra of fayalite heated in air for three days at temperatures between 700 °C and 1150 °C. The infra-red absorption spectra were recorded in the 1300 to 500 cm^{-1} region on a Perkin Elmer Model 337 grating infra-red spectrometer at sample concentrations of 1·2 mg in 200 mg of KBr.

The spectra obtained are shown in fig. 4. At 700 and 750 °C some of the fayalite remains unoxidized, but for all other temperatures the whole spectrum can be attributed to silica (the absorption peaks for hematite and spinel occur between 400 and 600 cm^{-1}).

At the lower temperatures, the peaks are very broad and the spectrum resembles that of silica glass. As the temperature is raised the peaks at approximately 1100 and 800 cm^{-1} sharpen, and at 1050 °C a small blip (marked q), which can be attributed to quartz, appears at about 780 cm^{-1}.

At higher temperatures two peaks characteristic of cristobalite appear (marked c).

Iron-oxide–silica intergrowths. Whereas single-crystal X-ray diffraction gives an overall picture of a solid state reaction in terms of the phases produced and their topotactic relationship to the host, it cannot, in general, be used to determine the mechanism of nucleation and growth of the phases. Transmission electron microscopy allows a high-resolution image to be correlated with the diffraction pattern from a region of the sample as small as 5×10^{-14} cm^3. It is therefore possible to isolate and examine the separate phases involved in the reaction; specifically this allows examination of the very early stages of phase transition.

The instrument used in the investigation was an A.E.I. EM-6G equipped with high-resolution dark-field facilities and a goniometer stage. Some specimens were heated in the furnace as thin slices of rock (about 0·5 mm thick) and then thinned by ion bombardment (Barber, 1970).[1] Other samples were heated as single crystals and crushed in absolute alcohol and a drop of the suspension was deposited on a carbon-coated electron-microscope grid.

Fig. 5*a* is a dark-field electron micrograph (taken with a matrix reflection) of the olivine containing 47 mol % fayalite that was heated for eight days at 650 °C (X-ray diffraction indicates that a very small amount of hematite is formed during this heat treatment). The micrograph shows small two-phase particles, which have nucleated on an array of parallel dislocations.

The reaction is a cellular one in which needles of hematite approximately 50 Å apart grow into the matrix (fig. 5*b*) separated by regions that appear to be amorphous silica (diffraction patterns from the two-phase precipitate indicate that only one crystalline phase, namely hematite, is present). Although the orientation of the oxide

[1] The author is greatly indebted to Dr. D. J. Barber of the University of Essex for preparation of these samples.

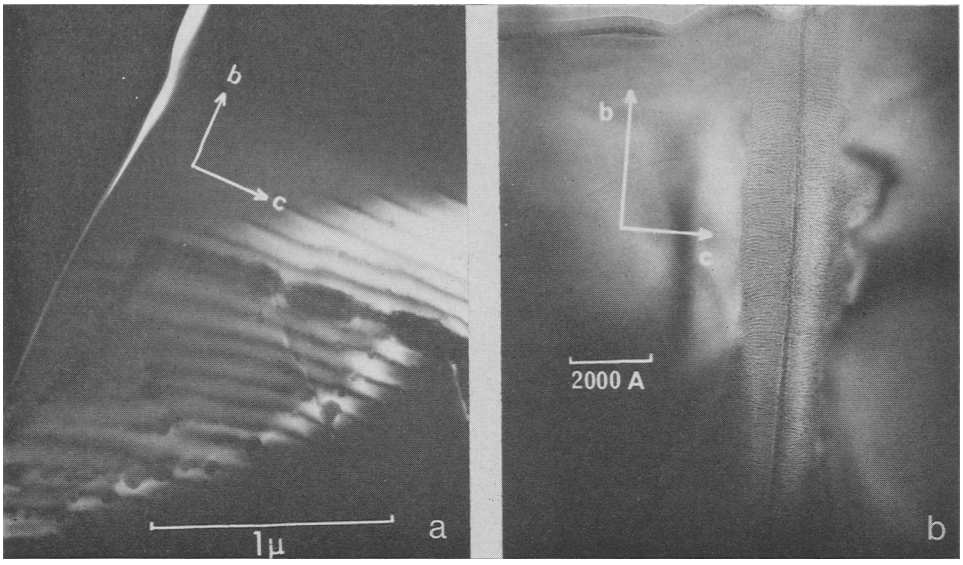

FIG. 5 *a*, Dark-field electron micrograph of 47 mol % fayalite olivine heated for eight days at 650 °C. Spherical particles of hematite–silica intergrowths have nucleated on dislocations and in the centre of the photograph have grown into a cylindrical colony. Specimen prepared by ion bombardment. *b*, Another area of the same single crystal showing needle-like hematite growing from a dislocation.

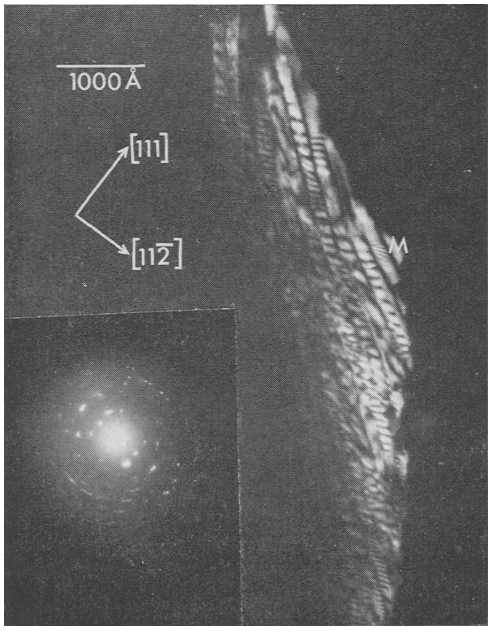

FIG. 6. Dark-field electron micrograph of fayalite heated for three days at 800 °C, three days at 900 °C, and one day at 950 °C. Needle-like spinel precipitates show arrays of misfit dislocations and, in one case, a moiré pattern M.

in the olivine is topotactic, the direction of the axes of the needle-like precipitates is determined by the orientation of the nucleating dislocation. The needles appear to radiate from the dislocation line forming a cylindrical colony. The randomness of the needle-axis direction is unusual and may be related to the fact that the second phase is amorphous and can accommodate stress more easily than could a well-crystallized precipitate.

Electron microscopy shows that at temperatures below 1000 °C the spinel-like phase also grows as needles (fig. 6). The average spacing of the precipitates is about 150 Å and they show the same randomness of axial direction as the hematite precipitates.

When the direction of the operating reflection is parallel to the needle axis a complex banded contrast can be seen in the oxide phases. The banding is always approximately perpendicular to

the needle axis. Some of the fringe contrast arises from moiré patterns produced by the overlap of two needles with slightly different orientations (fig. 6); in other cases the fringes are extinction contours in the highly buckled needles, but in the majority of cases they are produced by arrays of dislocations. A similar contrast has been observed in metal alloys by Weatherly and Nicholson (1968) on semi-coherent precipitates and on precipitates that had become completely non-coherent.

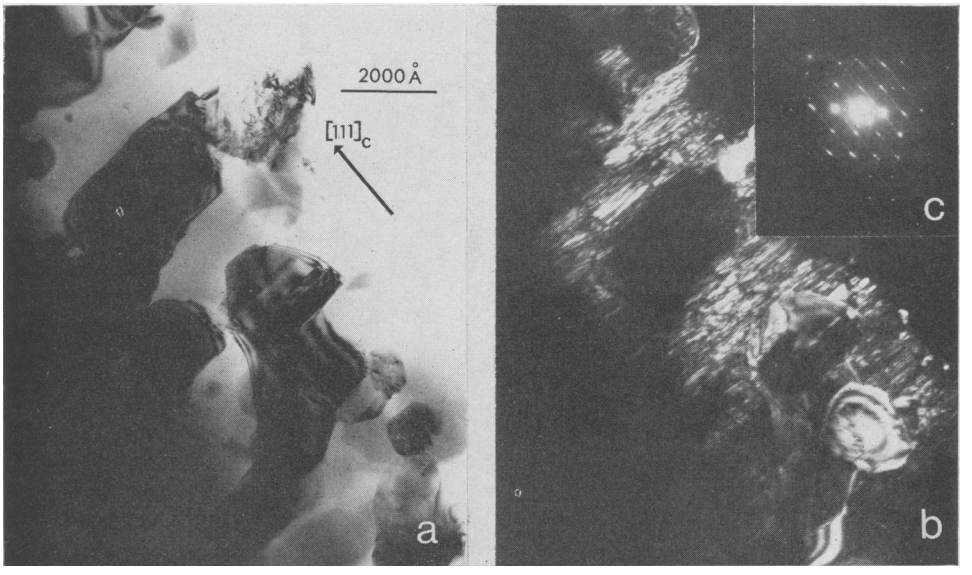

FIG. 7. *a*, Bright-field electron micrograph of a fayalite heated for three days at 1050 °C showing equiaxed grains of hematite in a matrix of poorly crystalline silica. *b*, Dark-field micrograph of the same area showing extensive faulting in the silica. *c*, Diffraction pattern from the silica. It corresponds more nearly to cristobalite than tridymite or quartz.

Christian (1965) has reviewed the dislocation structure at interfacial boundaries. In the case of a semi-coherent boundary, the most efficient relief of misfit is achieved by an array of parallel edge-dislocations with their Burgers vectors lying in the boundary plane. For a needle-shaped precipitate with a small misfit along the needle axis [*uvw*], the misfit can be relieved by prismatic loops with a Burgers vector in the [*uvw*] direction. It is probable that the dislocation structure present in the oxide precipitates in olivine consists of such prismatic loops, although as yet it has not been possible to prove this proposal by diffraction experiments.

The existence of misfit dislocations at the interface between the oxides and the amorphous silica that are precipitated from oxidized olivines shows that, at least in the early stages of the reaction, there is some degree of continuity across the inter-phase boundary. As the size of the oxide precipitates does not change significantly between 650 and 950 °C for a fixed time of heating, the change in the diffuseness of the X-ray reflections is probably due to a gradual decrease in structural continuity between the two phases. Complete loss of coherency possibly coincides with the crystallization of

the silica at 900 °C (this is the temperature at which the X-ray reflections become noticeably sharper). Diffuseness of the reflections at lower temperatures can be accounted for by the high state of strain in the oxide precipitates and possibly by some substitutional disorder, especially near the oxide–silica interface. A detailed investigation of the loss of coherency in the oxide–silica intergrowth is in progress.

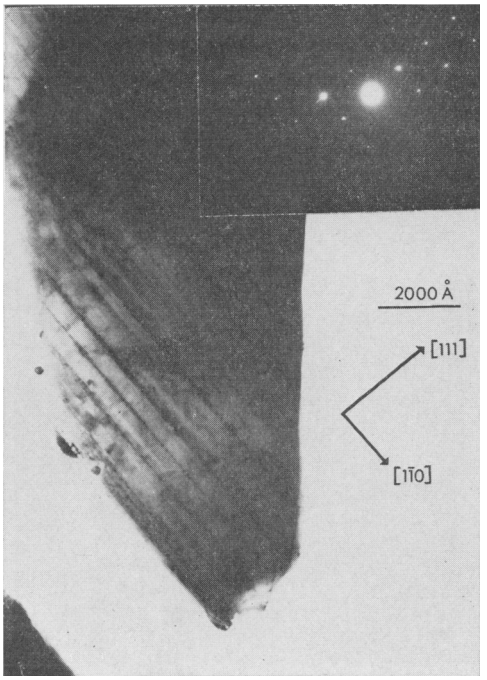

FIG. 8. Electron micrograph and diffraction pattern of a grain of cristobalite formed from fayalite heated for three days at 1150 °C. The 'tweed' contrast is due to coherent microtwin domains on {110} planes, which form as the sample is quenched through the $\beta \longrightarrow \alpha$ cristobalite transition (Champness, 1968). The diffraction pattern shows evidence of stacking faults on {111}.

X-ray diffraction indicates that recrystallization of the oxide phases occurs at 1000 °C and the silica also crystallizes rapidly at this temperature. Electron micrographs of fayalite heated at 1000 °C and above show equiaxed strain-free grains of oxide, the size of which increases with increasing temperature (fig. 7). After oxidation for three days at 1000 and 1050 °C the matrix silica shows a very disordered diffraction pattern (fig. 7*c*) and dark field micrographs indicate an extremely high density of stacking faults and dislocations (fig. 7*b*).

As the temperature of crystallization is increased (or the sample is annealed at constant temperature), the structural regularity of the silica improves. However, even after heating for three days at 1150 °C the cristobalite-like phase still contains stacking faults (fig. 8) and twins on {111} planes.

Both cristobalite and tridymite can be described in terms of stacking of sheets of six-membered rings of SiO_4 tetrahedra parallel to $\{111\}_c$ and $\{001\}_t$; the stacking in cristobalite resembles cubic close-packing and that in tridymite resembles hexagonal close-packing. 'Mistakes' in the sequence of planes parallel to {111} of cristobalite can be considered as forming a small region of tridymite or a small twinned region depending on the nature of the stacking mistakes. The faults have a stacking vector of $a/3[\bar{1}\bar{1}2]$ and this results in streaks in reciprocal space parallel to $g(111)_c$ for reflections $(h+k+l) \neq 3n$. Such streaks have been observed in diffraction patterns from the cristobalite-like phase (Champness, 1968).

Formation of pyroxene

The MgO–SiO_2 equilibrium diagram shows that silica is unstable in the presence of forsterite, and therefore enstatite is to be expected as one of the reaction products of

the oxidation of forsteritic olivines. Though a small amount of a pyroxene-like phase is precipitated at lower temperatures in Mg-rich single crystals of olivine (though not in powders), silica is formed metastably and crystallizes at about 900 °C. However, as the reaction proceeds the silica and forsterite react to form more pyroxene (fig. 2*b*).

The metastable crystallization of silica in the presence of forsterite must be due to the intimate intergrowth that forms in the early stages of the reaction between the silica and the iron oxides. Oxidation occurs on the surface, presumably by the diffusion of Fe^{2+} ions through the oxygen framework to the reaction interface, where they become Fe^{3+}. Diffusion of Mg^{2+} ions must occur in the opposite direction in order to maintain local charge balance. Thus as the iron-oxide–silica intergrowth forms, the interior of the crystal becomes more forsteritic. It is only at temperatures where large-scale diffusion can take place that the forsterite and silica can react together to form enstatite.

Initially only two very faint and rather diffuse powder lines at approximately *d* 3·2 Å and *d* 2·9 Å can be detected from the pyroxene on single-crystal oscillation photographs. It is thus impossible to identify the structure with any of the enstatite polymorphs and would probably be meaningless to do so. On the other hand, forsteritic olivines heated at 1100 °C and above show three additional powder lines from the pyroxene and, as the lines are sharper and more intense at these temperatures, they can be measured with greater accuracy. Measurements show that the pyroxene corresponds more closely to protoenstatite than to either of the other two polymorphs.

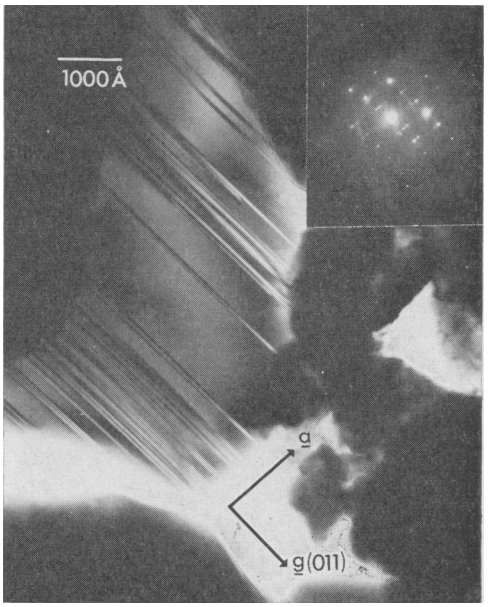

FIG. 9. Electron micrograph and diffraction pattern of a pyroxene grain from the 47 % fayalite specimen heated for three days at 1200 °C. It has stacking faults on (100) planes.

The pyroxene has been isolated in the electron microscope and fig. 9 shows a typical grain from the 47 % fayalite sample that was heated for three days at 1200 °C. The diffraction pattern shows that the phase is orthorhombic and leads to a value for *a* of about 9 Å. This confirms the X-ray result that the pyroxene resembles protoenstatite rather than orthoenstatite (which has an *a*-axis of about 18 Å).

The preferred orientation of the pyroxene with respect to the parent olivine is poor. Twelve reflections appear on the 3·17 Å powder line on oscillation photographs taken with c_{ol} or b_{ol} vertical, oscillating across a^* (fig. 2*b*). Measurement of the layer-line spacings showed that there are two orientations of the pyroxene with respect to the

olivine. These are: $(100)_{ol} \| (100)_p$, $b_{ol} \| c_p$, $c_{ol} \| b_p$, and $(100)_{ol} \| (100)_p$, $b_{ol} \| \pm[011]_p$, $c_{ol} \| \pm[01\bar{3}]_p$.

The oxygen ions in the (100) plane form imperfect hexagonal sheets and the b and [011] directions in these sheets are at approximately 60° and to some extent resemble the close-packed direction in olivine (fig. 3).

The cell dimensions calculated from the layer-line spacings compare well with the normal cell dimensions of protoenstatite.

At high oxidation temperatures the pyroxene is quite well crystalline; the electron-diffraction pattern in fig. 9 shows Kikuchi lines and the micrograph shows smooth extinction contours. However, there are numerous stacking faults on (100) planes.

The three common enstatite polymorphs have SiO_3 chains parallel to c, which are arranged in slabs parallel to (100). Successive slabs may be considered as related approximately by stacking vectors of $\pm c/3$ and the sequence in which these vectors occur gives rise to the different polymorphs. The simple relationship between the structures leads to the possibility of disordered structures. Evidence of disorder similar to that seen in the protoenstatite formed from olivine has been found by Brown and Smith (1963) in rapidly cooled enstatites.

Acknowledgements. The author wishes to thank Drs. S. O. Agrell and I. D. Muir for the provision of specimens. Drs. P. Gay and G. W. Lorimer provided helpful advice and criticism of specific aspects of the study. Part of the work was carried out while the author was in receipt of a Research Studentship from N.E.R.C. The electron microscope was provided for the Department of Geology, University of Manchester by N.E.R.C.

REFERENCES

BARBER (D. J.), 1970. *Journ. Materials Sci.* **5**, 1.
BOWEN (N. L.), SCHAIRER (J. F.), and POSNJAK (E.), 1933. *Amer. Journ. Sci.* **225**, 273.
BROWN (W. L.) and SMITH (J. V.), 1963. *Zeits. Krist.* **118**, 186.
CHAMPNESS (P. E.), 1968. Ph.D. Thesis, Cambridge University.
—— and GAY (P.), 1968. *Nature*, **218**, 157.
CHRISTIAN (J. W.), 1965. *Theory of Transformations in Metals and Alloys*, p. 331. Pergamon Press (London).
DEER (W. A.), HOWIE (R. A.), and ZUSSMAN (J.), 1962. *Rock-Forming Minerals*, **5**. Longmans (London).
GORGEU (A.), 1885. *Compt. Rend. Acad. Sci. Paris*, **98**, 1281.
HAGGERTY (S. E.) and BAKER (I.), 1967. *Contr. Min. Petr.* **16**, 233.
HOLGERSSON (S.), 1927. *Lunds Univ. Årsskrift*, **23**, No. 9.
HUGILL (W.) and GREEN (A. T.), 1938. *Trans. Brit. Ceram. Soc.* **37**, 279.
JAY (A. H.), 1944. *Min. Mag.* **27**, 54.
KOLTERMANN (M.), 1962. *Neues Jahrb. Min. Monatsh.* 181.
—— and MUELLER (K. H.), 1963. *Ber. deutsch. keram. Ges.* **40**, 20.
POSNJAK (E.), 1930. *Amer. Journ. Sci.* ser. 5, **19**, 67.
TILLEY (C. E.), 1952. Ibid. **Bowen vol.** 529.
VENABLES (J. A.), 1962. *Phil. Mag.* **7**, 35.
WEATHERLY (G. C.) and NICHOLSON (R. B.), 1968. Ibid. **17**, 801.
WEISKIRCHNER (W.), 1958. *Rend. Soc. Min. Ital.* **14**, 355.
YODER (H. S.) and SAHAMA (Th. G.), 1957. *Amer. Min.* **42**, 475.

[*Manuscript received 18 March 1970*]